

- Supporting Information -

**Ni-WSe₂ Nanostructures as an Efficient Catalysts for
Electrochemical Hydrogen Evolution Reaction (HER) in acidic and
alkaline media**

Sunil R. Kadam^{1,2}, Andrey N. Enyashin^{3,4} Lothar Houben⁵ Ronen Bar-Ziv⁶, Maya Bar-Sadan,^{1,2}*

¹ *Ben-Gurion University of the Negev, Department of Chemistry, Beer-Sheva, Israel.*

² *Ilse Katz Institute for Nanoscale Science and Technology, Ben Gurion University, Beer Sheva Israel.*

³ *Institute of Solid State Chemistry UB RAS, 620990 Ekaterinburg, Russian Federation*

⁴ *Ural Federal University, Institute of Natural Sciences and Mathematics, 620083 Ekaterinburg, Russian Federation*

⁵ *Department of Chemical Research Support, Weizmann Institute of Science, Rehovot, Israel*

⁶ *Chemistry Department, Nuclear Research Center-Negev (NRCN), Beer Sheva 84190, Israel.*

E-mail: barsadan@bgu.ac.il

1. Experimental section

Materials

All the chemicals were used as received without further purification. Ammonium metatungstate hydrate ((NH₄)₆H₂W₁₂O₄₀·xH₂O) (STREM chemicals), Selenium powder (Se) (Acros organics), Nickel (II) acetylacetonate (Acros organics), Iron (III) acetylacetonate (STREM Chemicals Inc.), Cobalt (II) 2,4-pentanedionate (Alfa Aesar), Sodium Niobate (Acros organics), Zirconium (IV) chloride (Aldrich), Oleylamine (Aldrich) and 1-Octadecene (Aldrich) with (Purity 99.9 %). The water used for washing was de-ionized water (DW) that was passed through a Milli-Q column by Millipore, with final resistance of 18.2 MΩ cm.

Synthesis of pristine and doped WSe₂ catalyst

Pristine WSe₂ was synthesized by simple colloidal method. All the reactions were performed using standard Schlenk line technique. At first, ODE-Se precursor was prepared in a 100 mL three neck round bottom (RB) flask by adding 1 mmol selenium powder (79 mg) in 20 mL ODE. The mixture was degassed under vacuum at 110 °C for 30 min, then the vacuum was stopped and the RB flask was backfilled with N₂ gas, heated to 200 °C and maintained at this temperature for 2 hrs to obtain light-yellow coloured Se-ODE precursor solution. Further, in another 100 mL three-neck RB flask, 0.2 mmol of ammonium metatungstate hydrate ((NH₄)₆H₂W₁₂O₄₀·xH₂O) were mixed with 20 mL of oleylamine. The mixture was degassed under vacuum at 110 °C for 30 min until a clear solution was obtained. Then the RB was backfilled with N₂ gas and 0.4 mmol of Se-ODE precursor solution (8 mL) were added dropwise using a syringe pump with constant stirring. The total volume of the reaction mixture was 28 mL. Further, the reaction temperature was slowly increased to 300°C at 5 °C/min rate and maintained for the next 3 hours. After completion of the reaction, the heating mantle was removed and the reaction mixture was allowed to cool naturally. The final product was collected by centrifuging and washing twice with toluene, ethanol and acetone followed by vacuum drying. The dried powder sample was annealed under N₂ atmosphere at 250 °C for 3 hours in order to remove the ligands and increase the crystallinity. Doped WSe₂ samples were synthesized by the same procedure except for substitution with the doping element in the desired ratio.

Electrode preparation and Electrochemical HER Measurements

Ink for the working electrodes was prepared by dispersing 2 mg of the catalyst and 1 mg Vulcan carbon black in 550 µl of Nafion solution (prepared by mixing of 2000 µl water, 500 µl ethanol and 150 µl Nafion solution (5%)). The ink was homogenized by bath ultra-sonication for 2 min followed by probe sonication (QSONICA 125 W probe sonicator) at 40% amplitude in an interval mode of 15:5 seconds on:off cycle for additional 5 min. 3 mm glassy carbon (GC) working electrode was polished to a mirror-like finish using alumina slurry and then 20 µl of the homogeneous ink was drop casted onto the GC electrode to form a final loading of ~1 mg cm⁻² and kept overnight. Standard three electrode system was used for all the electrochemical measurements. Graphite rod, saturated Ag/AgCl and glassy carbon electrode coated with the WSe₂ catalyst were used as the counter, reference and working electrodes, respectively. Polarization curves were recorded on an Ivium Technology Vertex Potentiostat/Galvanostat (V74606) and analyzed using the Ivium Soft program. The electrochemical HER measurements were performed in Argon-saturated 0.5 M H₂SO₄ or 0.5 M KOH solutions at room temperature. The electrolyte was bubbled with Ar gas for 15 minutes prior to the measurements in order to remove dissolved gases from the solution. Each electrode was pre-treated with 12 cyclic voltammetry (CV) cycles between 0 V to -0.7 V (vs. RHE) at a scan rate of 100 mV S⁻¹. Polarization curves were recorded at a scan rate of 10 mV s⁻¹ over the same potential range. During the electrochemical measurements the head

space of the cell was continuously purged with Ar gas. All measurements were referred to the reversible hydrogen electrode (RHE) by using the relationship: $E_{(RHE)} = E_{(Ag/AgCl)} + E^0_{(Ag/AgCl)} + 0.059V \times pH$. To characterize the materials directly before and after the catalytic reaction, we prepared another set of electrodes without carbon black (which complicates the analysis). The new set of electrodes was prepared by dispersing 3 mg of 10% Ni-WSe₂ in 300 μ l of the following solution: 2000 μ l water, 500 μ l ethanol and 150 μ l Nafion solution (5%). The electrodes were cycled for 3000 continuous CV cycles (from 0 to -0.3 V RHE) in both acidic and alkaline media.

Materials Characterization

The crystallographic phase of the sample was identified by Panalytical Empyrean powder X-ray diffractometer equipped with a position-sensitive X'Celerator detector using Cu K α radiation ($\lambda = 1.5405 \text{ \AA}$) operated at 40 kV and 30 mA. The surface morphologies of the synthesized sample were investigated by JEOL JSM-7400F ultrahigh resolution cold FEG-SEM. The sample for SEM was prepared by dispersing the powder in ethanol, followed by sonication in an ultrasonic bath for 1 min and then drop-casting the dispersion on a silicon wafer. The images were recorded at 2 kV acceleration voltage at 3–4 mm sample distance. High-resolution transmission electron microscopy (HRTEM) images were acquired on a 200 kV JEOL 2100F instrument. Samples were prepared by dispersing the powder in ethanol, followed by sonication in an ultrasonic bath for 2 min. and then drop-casting the dispersion on a carbon coated copper grid and by subsequent drying in a vacuum. XPS data were collected using an X-ray photoelectron spectrometer ESCALAB 250 ultrahigh vacuum (1×10^{-9} bar) apparatus with an Al K α X-ray source and a monochromator. Room temperature Raman spectroscopy were performed using a LabRAM HR Evolution Raman spectrometer with a laser wavelength of 532 nm in the back-scattering geometry laser power on the sample was 5 mW with a laser spot size 2 μ m.

TEM Microscopy

High-resolution transmission electron microscopy images and analytical data were recorded in a double aberration-corrected Themis Z microscope (Thermo Fisher Scientific Electron Microscopy Solutions, Hillsboro, USA) equipped with a high-brightness FEG. Accelerating voltages of 200 kV, 80 kV and 40 kV were used. Aberration-corrected TEM images were recorded on a Gatan OneView CMOS camera (Gatan Inc., Pleasanton, USA). High-angle-annular dark-field (HAADF) scanning transmission electron microscopy (STEM) images were recorded with a Fischione Model 3000 detector with a semi-convergence angle of 30 mrad, a probe current of typically 50 pA, and an inner collection angle of 70.0 mrad. EDS hyperspectral data were obtained with a Super-X G2 four-segment SDD detector with a probe semi-convergence angle of 30 mrad, a beam current of approximately 200 pA. The EDS hyperspectral data were quantified with the Velox software (Thermo Fisher Scientific Electron Microscopy Solutions, Hillsboro, USA), through background subtraction and spectrum deconvolution.

EEL maps were recorded on a Gatan Quantum GIF 966ERS energy loss spectrometer (Gatan Inc., Pleasanton, USA) with an Ultrascan1000 CCD camera. The EEL maps were recorded with a STEM probe with a semi-convergence angle of 30 mrad and a beam current of 100 pA. The outer semi-collection angle of the spectrometer was 50 mrad. DigitalMicrograph (Gatan Inc., Pleasanton, USA) was used for the quantification of the EEL maps.

Computational Details

Quantum-chemical calculations were performed within the DFT approach as implemented in SIESTA 4.0 package.¹ Generalized Gradient Approximation (GGA) in the Perdew-Burke-Ernzerhof (PBE) parametrization was used for description of exchange-correlation potential. The core electrons were treated within the frozen core approximation, applying norm-conserving Troullier–Martins pseudopotentials.² The valence shells were taken as $5d5s16p0$ for W, $3d84s24p0$ for Ni, $4s24p4$ for Se and $1s1$ for H. The double- ζ basis set was used for description of valence orbitals. A cutoff of 15 Å was used for k -point sampling.³ The k -point mesh was generated by the method of Monkhorst and Pack. The real-space grid used for the numerical integrations was set to correspond to the energy cutoff of 300 Ry. The calculations were performed using variable-cell and atomic position relaxations, with convergence criteria corresponding to the maximum residual stress of 0.1 GPa for each component of the stress tensor, and the maximum residual force component of 0.05 eV/Å. A vacuum region of 20 Å was introduced along the out-of-plane direction to eliminate spurious interactions among periodic images of 2D-structures or along all three directions for individual molecules. The 4×4 supercells for both WSe₂- and NiSe-based substrates were employed as the main models for the studies of Ni alloying, NiSe deposition and H adsorption.

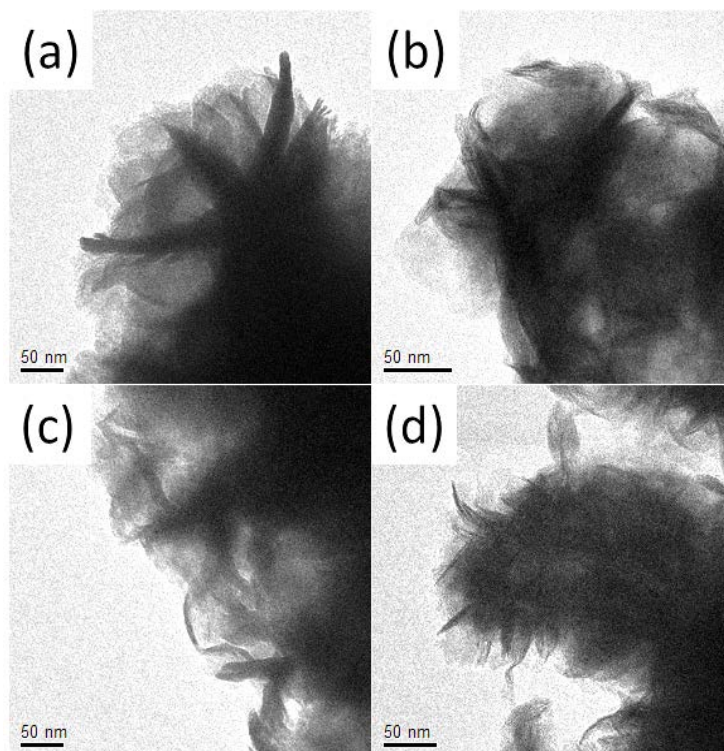


Figure S1. TEM images of: Pristine WSe₂ (a), 3% Ni doped WSe₂ (b) 5% Ni doped WSe₂ (c), 10% Ni doped WSe₂ (d).

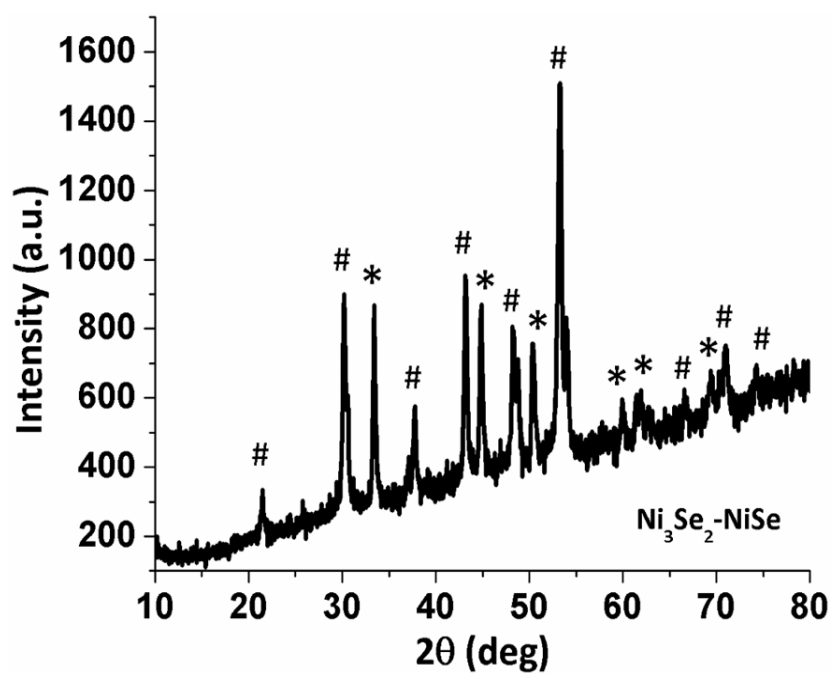


Figure S2. XRD pattern of Ni₃Se₂-NiSe sample synthesized at identical conditions, the Rhombohedral Ni₃Se₂ peaks indicated by # and hexagonal NiSe indicated by *.

Table S1: Peak area obtained for W, Se and Ni from X-ray photoelectron spectroscopy

		Pristine WSe ₂ (Peak Area)	3% Ni-WSe ₂ (Peak Area)	5% Ni-WSe ₂ (Peak Area)	10% Ni-WSe ₂ (Peak Area)
W	4f _{7/2}	32.05	32.10	32.26	32.34
	4f _{5/2}	34.15	34.16	34.36	34.44
	4f _{7/2}	35.76	35.68	35.82	35.90
	4f _{5/2}	37.86	37.78	37.92	38.00
Se	3d _{5/2}	54.33	54.37	54.52	54.59
	3d _{3/2}	55.13	55.17	55.31	55.39
Ni	2P			854.61	854.61

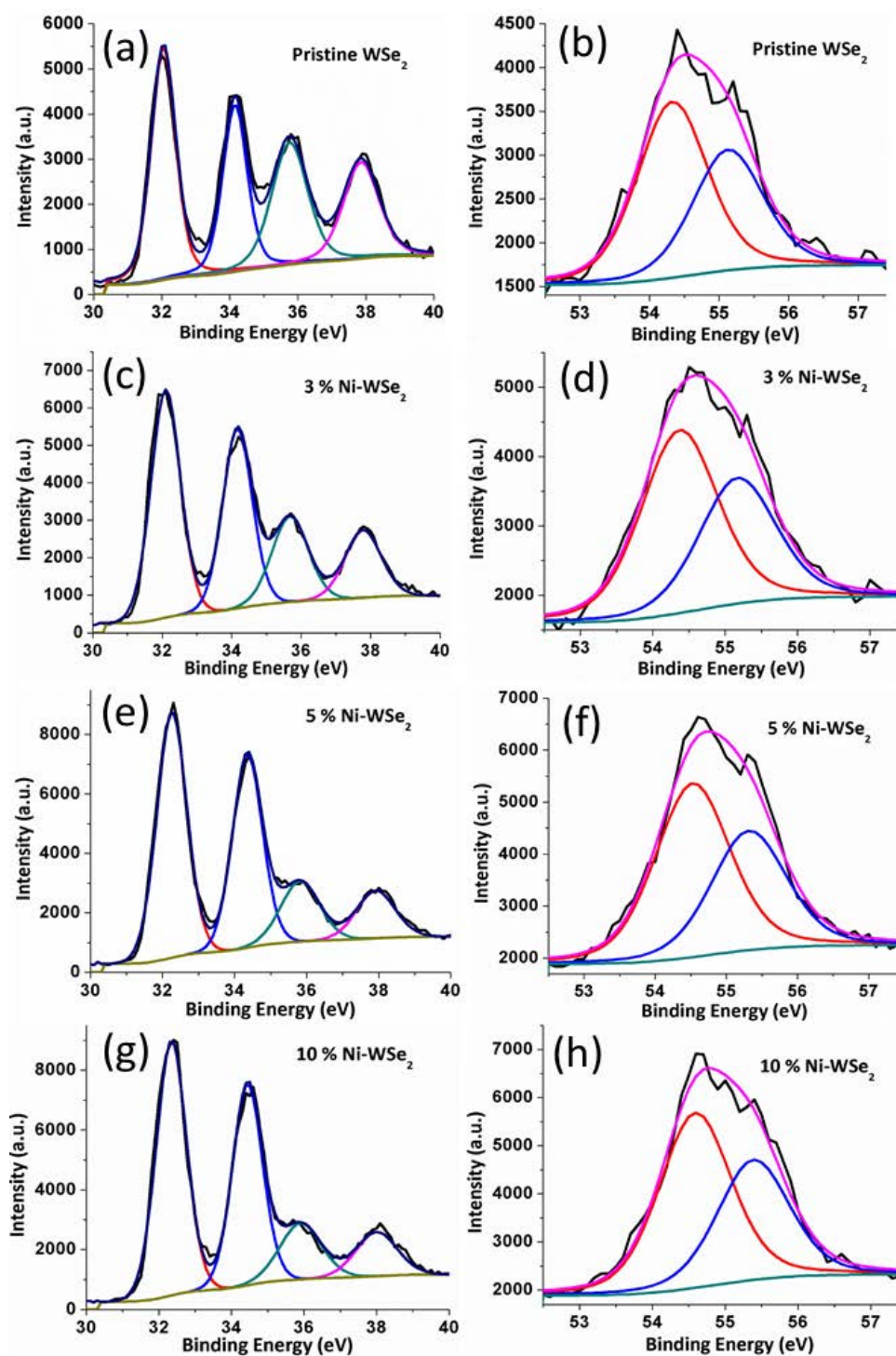


Figure S3. Deconvoluted X-ray photoelectron spectra of (a,) W 4f and (b) se 3d for pristine WSe₂, (c) W 4f and (d) se 3d for 3 % Ni-doped WSe₂, (e) W 4f and (f) se 3d for 5 % Ni-doped WSe₂, (g) W 4f and (h) se 3d for 10 % Ni-doped WSe₂ sample.

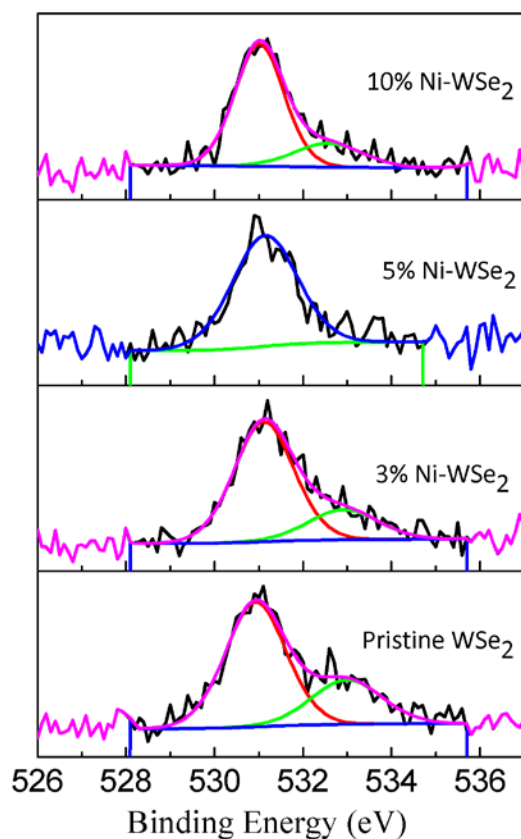


Figure S4. X-ray photoelectron spectra of O 1s for pristine WSe₂, 3 %, 5 % and 10 % Ni-doped WSe₂.

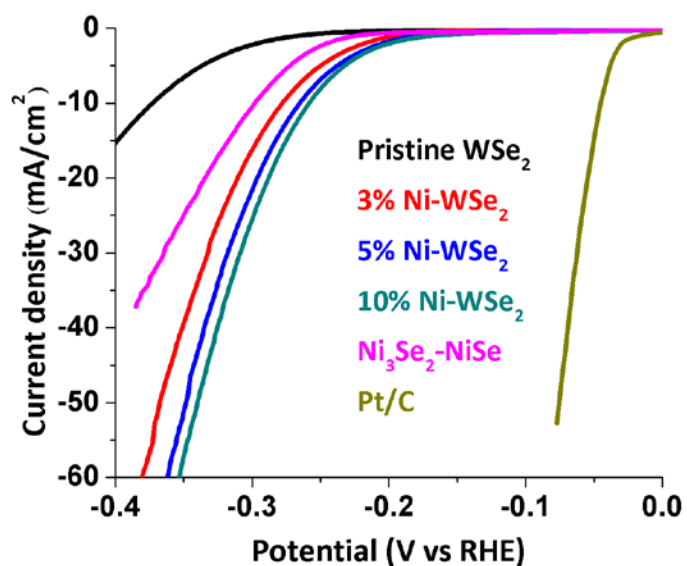
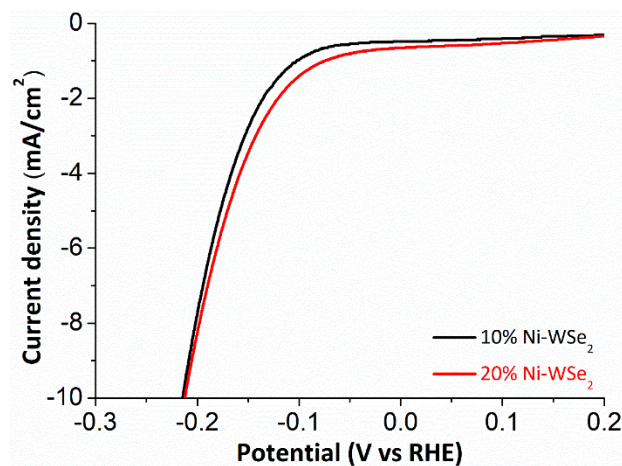


Figure S5 (a) HER polarization curves at high current densities of the pristine WSe₂ along with 3 %, 5 % and 10 % Ni-doped WSe₂ sample in 0.5 M H₂SO₄.

Table S2: Electrochemical HER performance of present work along with previous reports.

No.	Sample	Electrolyte	Over Potential (V), η at 10 mA cm ⁻²	Tafel slope (mV dec ⁻¹)	Ref
1	WSe ₂ Nanosheets	0.5 M H ₂ SO ₄	-0.760		4
2	WSe ₂	0.5 M H ₂ SO ₄	-0.850	176	5
3	V-doped WSe ₂	0.5 M H ₂ SO ₄	-0.750	113	
4	Nb-doped WSe ₂	0.5 M H ₂ SO ₄	-0.750	124	
5	Ta-doped WSe ₂	0.5 M H ₂ SO ₄	-0.750	136	
6	WSe ₂ Nanotube supported on carbon fibers	1 M H ₂ SO ₄	-0.350	99	6
7	2D Nanosheets supported on carbon fibers	0.5 M H ₂ SO ₄	-0.300	77.4	7
8	Exfoliated WSe ₂ Nanosheets	0.5 M H ₂ SO ₄	-0.800	120	8
9	WSe ₂ nanostructure	0.5 M H ₂ SO ₄	-0.307	126	9
10	WSe ₂ /rGO	0.5 M H ₂ SO ₄	-0.180	64	10
11	Ni-doped WSe ₂ petalled nanostructures	0.5 M H ₂ SO ₄	-0.259	86	Present Work
		0.5 M KOH	-0.215	109	

**Figure S6.** Comparison of the catalytic activity towards HER of the 10 % and 20% Ni-doped WSe₂ in 0.5 M KOH.

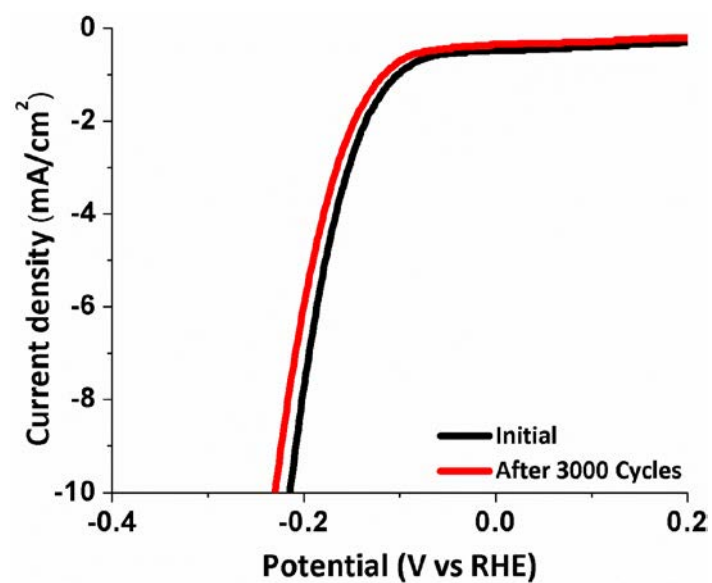


Figure S7. Functional Stability test of 10 % Ni-doped WSe₂ sample in 0.5 M KOH

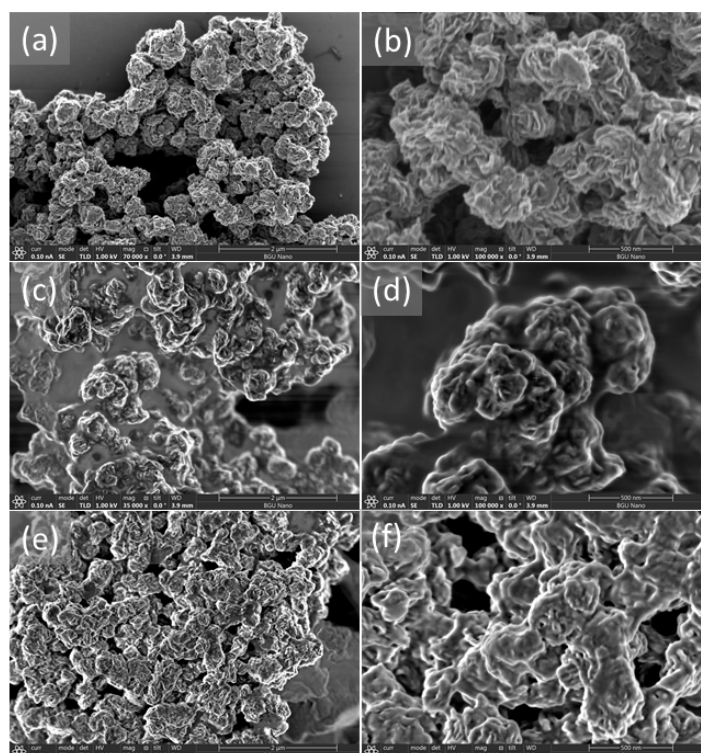


Figure S8. SEM images of 10% Ni-WSe₂ sample: (a,b) before stability study (c,d) after stability performed in 0.5 M H₂SO₄ (e,f) after stability performed in 0.5 M KOH.

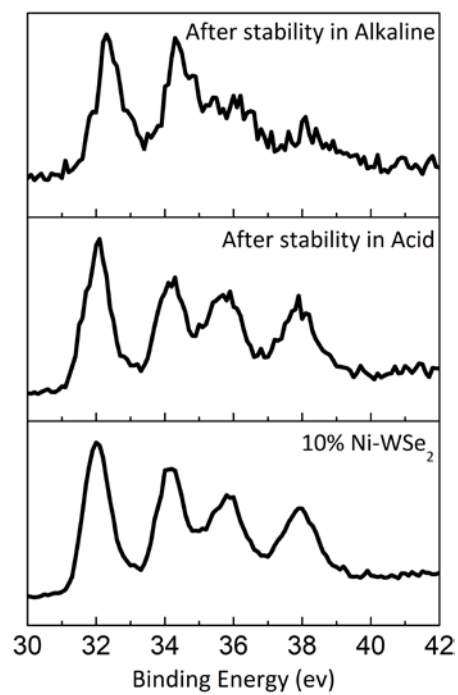


Figure S9. X-ray photoelectron spectra of W 4f for 10 % Ni-doped WSe₂ before the stability study and after the stability in acid and alkaline media.

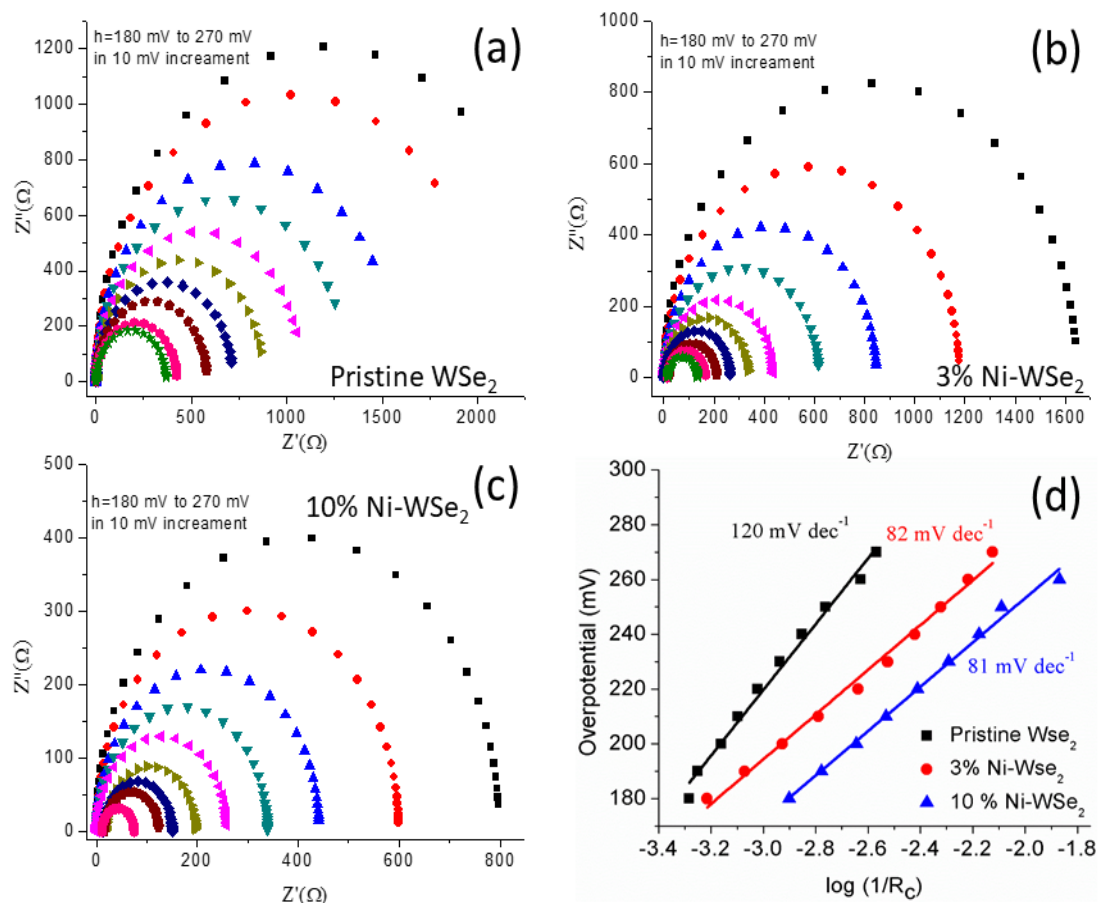


Figure S10. (a) EIS measurements of Pristine WSe₂ (b) EIS measurements of 3 % Ni-Wse₂ (c) EIS measurement of 10 % Ni doped Wse₂ and (d) Tafel analysis from the Nyquist plots of impedance data of pristine WSe₂, 3% Ni-WSe₂ and 10 % Ni-WSe₂.

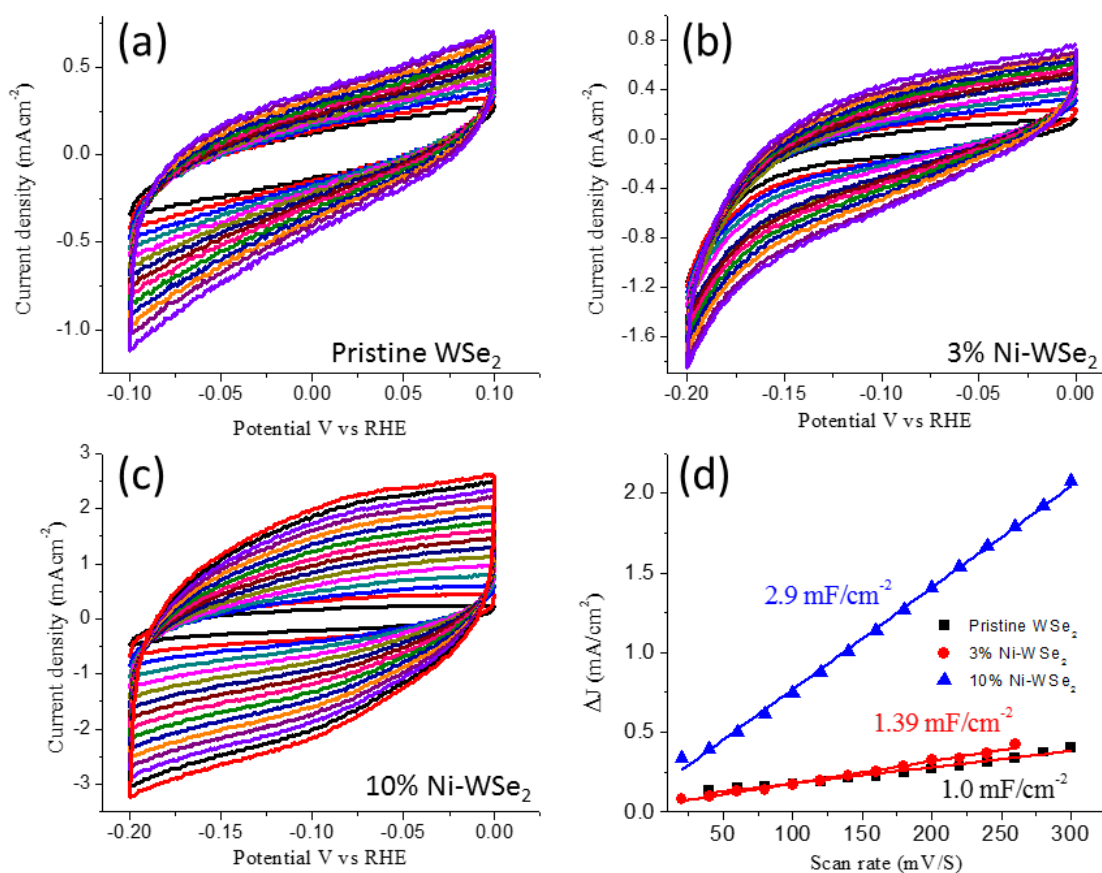
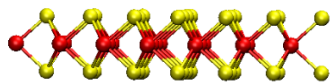
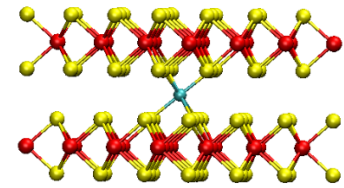
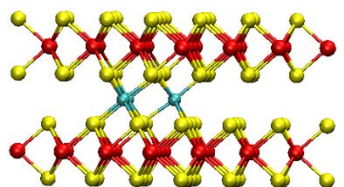
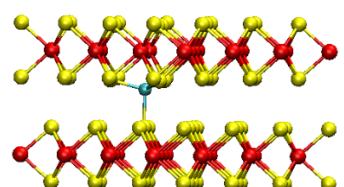
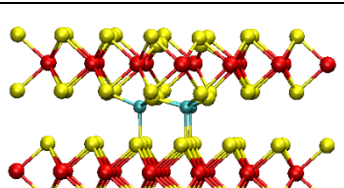
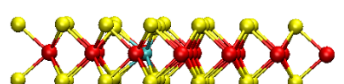
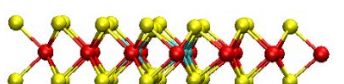
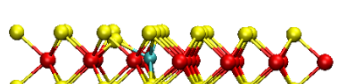


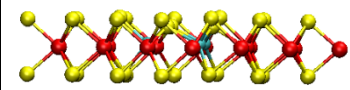
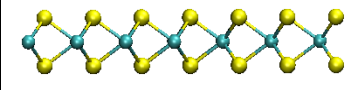
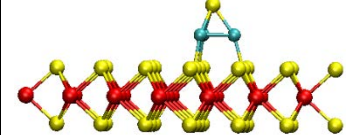
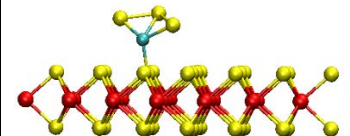
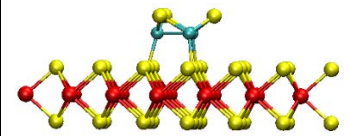
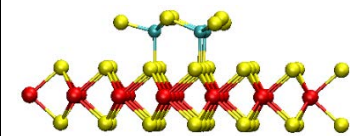
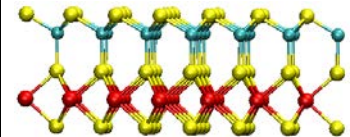
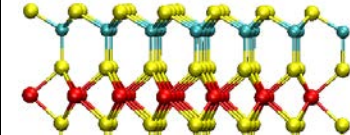
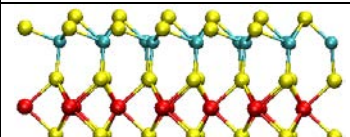
Figure S11. (a-c) Cyclic voltammograms measured in non-faradaic potential region of 0.10 to -0.10 V vs. RHE at various scan rates for Pristine WSe₂ and in the region of 0.0 to -0.20 V vs. RHE for 3% and 10% Ni-WSe₂ (d) the corresponding linear fitting of the capacitive currents (the difference between anodic and cathodic currents, Δj) vs. scan rates to estimate the double layer capacitance (C_{dl}) for pristine WSe₂, 3% and 10% Ni-WSe₂.

The measured capacitance values of the samples can be converted into **electrochemical active surface area (ECSA)** using a specific capacitance of flat standard with 1cm² of real surface area. By taking the specific capacitance value C_s for an ideally flat standard electrode into account, $C_s = 0.040 \text{ mF cm}^{-2}$, one can calculate $ECSA = C_{dl}/C_s$.

$$ECSA = \frac{\text{Specific Capacitance (mF cm}^{-2}\text{)}}{0.04 \text{ mF cm}^{-2}_{ECSA}}$$

Table S3. Formation energies ΔE for different models of Ni-WSe₂ nanostructures and single H-atom adsorption energies ΔG_H (according to equation 1 with correction +0.24 eV according to ref⁹). DFT calculations.

Description of the model	DFT-optimized structure	Formation energy ΔE , eV/Ni-atom	Corrected hydrogen adsorption energy ΔG_H , eV/H-atom
single layer WSe ₂		+0.33 (per WSe ₂) +34.9 meV/Å ²	+2.49
intercalation by single Ni-atom		+10.80	-
intercalation by three-atom Ni-cluster		+5.85	-
intercalation by single Ni-atom + single W-atom vacancy		+11.65	-
intercalation by three-atom Ni-cluster + three W-atom vacancies		+5.37	-
doping by single Ni-atom		+7.48	+0.09 (onto Se-Ni) +1.28 (onto Se-W)
doping by three-atom Ni-cluster		+2.92	-
doping by single Ni-atom + single Se-atom vacancy		+9.02	-

doping by three-atom Ni-cluster + three Se-atom vacancies		+3.96	-
NiSe ₂ layer (complete substitution of W in WSe ₂ layer)		+0.87	-
chemisorption of Ni ₃ Se cluster		+5.10	+1.29 (onto Se-Ni) +1.91 (onto Se-W)
chemisorption of NiSe ₃ cluster		+7.79	-
chemisorption of Ni ₃ Se ₃ cluster		+3.92	-0.30 (onto Se-Ni) +1.97 (onto Se-W)
chemisorption of Ni ₃ Se ₆ cluster		+3.84	-0.78 (onto Se(1)-Ni) -0.22 (onto Se(2)-Ni) +1.82 (onto Se-W)
NiSe single layer grafted onto WSe ₂ single layer		+1.09	-1.25 (onto Se-Ni) +2.06 (onto Se-W)
two NiSe single layers grafted onto WSe ₂ single layer		+0.92	-0.24
NiSe single layer grafted onto WSe ₂ single layer (2a×2a reconstruction)		+0.99	+0.24 (onto Se-Ni) +0.21 (onto Se-Ni) +2.09 (onto Se-W)

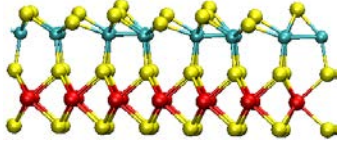
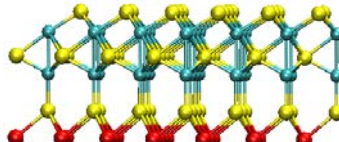
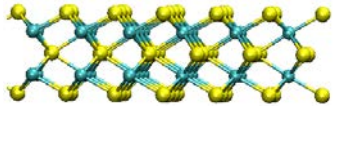
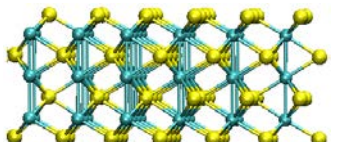
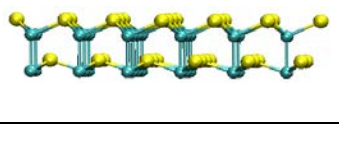
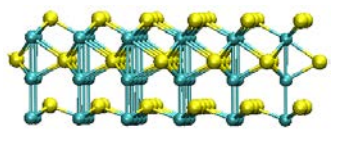
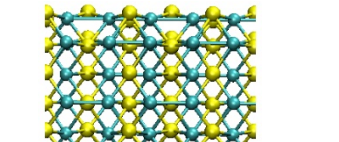
NiSe single layer grafted onto WSe ₂ single layer (3a×2a reconstruction)		+0.96	+1.66 (onto Se-Ni) +0.21 (onto Se-Ni) +0.72 (onto Se-Ni) +2.04 (onto Se-W)
NiSe double layer grafted onto WSe ₂ single layer		+0.69	+0.91 (onto Se-Ni) +2.10 (onto Se-W)
slab(001) Se(NiSe) ₂ non-polar Se-saturated		-0.36 -31.9 meV/Å ²	+0.17
slab(001) Se(NiSe) ₃ non-polar Se-saturated		-0.33 -43.8 meV/Å ²	+0.08
slab(001) (NiSe) ₂ polar non-saturated		+1.03 +91.1 meV/Å ²	-1.18 (onto Se) -0.45 (onto Ni)
slab(001) (NiSe) ₃ polar non-saturated		+0.68 +90.7 meV/Å ²	-
slab(100) (NiSe) ₃ non-polar non-saturated		+1.02 +142.1 meV/Å ²	+0.25

Table S4. Elemental composition of pristine and doped WSe₂ by SEM EDS.

	Pristine WSe ₂	3% Ni-WSe ₂	5% Ni-WSe ₂	10% Ni-WSe ₂
At% of Se	29.7	36.3	37.5	38.8
At% of W	15.8	16.9	18.0	17.9
At% of Ni		1.0	1.3	2.0
Overall stoichiometry	WSe ₂	(Ni _{0.05} W _{0.95})Se _{2.1}	(Ni _{0.07} W _{0.93})Se ₂	(Ni _{0.11} W _{0.89})Se ₂

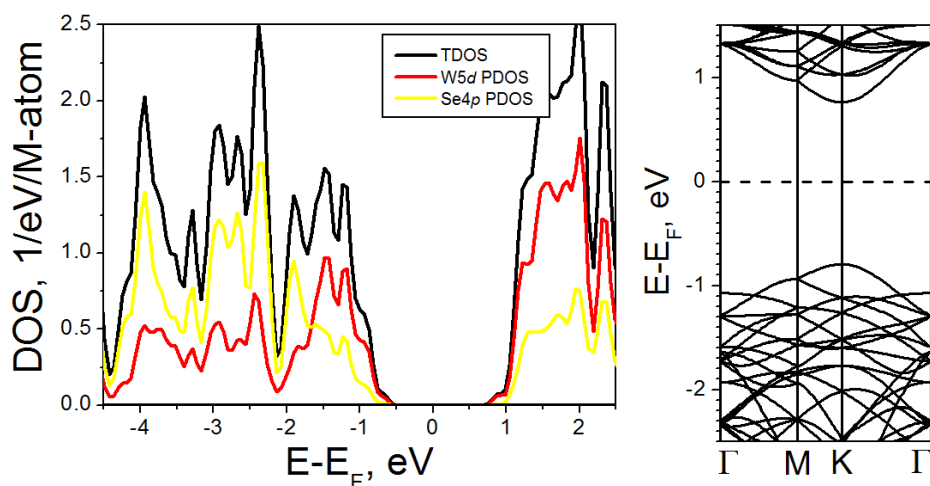


Figure S12. Electronic densities-of-states (DOS) and band structure for pristine WSe₂ monolayer. DFT calculations.

References

- Ordejón, P.; Artacho, E.; Soler, J. M., Self-consistent order-N density-functional calculations for very large systems. *Phys. Rev. B* **1996**, *53* (16), R10441-R10444.
- Troullier, N.; Martins, J. L., Efficient pseudopotentials for plane-wave calculations. *Phys. Rev. B* **1991**, *43* (3), 1993-2006.
- Moreno, J.; Soler, J. M., Optimal meshes for integrals in real- and reciprocal-space unit cells. *Phys. Rev. B* **1992**, *45* (24), 13891-13898.
- Sun, Y.; Zhang, X.; Mao, B.; Cao, M., Controllable selenium vacancy engineering in basal planes of mechanically exfoliated WSe₂ monolayer nanosheets for efficient electrocatalytic hydrogen evolution. *Chem. Commun.* **2016**, *52* (99), 14266-14269.
- Chia, X.; Sutrisnoh, N. A. A.; Sofer, Z.; Luxa, J.; Pumera, M., Morphological Effects and Stabilization of the Metallic 1T Phase in Layered V-, Nb-, and Ta-Doped WSe₂ for Electrocatalysis. *Chem. Eur. J.* **2018**, *24* (13), 3199-3208.
- Xu, K.; Wang, F.; Wang, Z.; Zhan, X.; Wang, Q.; Cheng, Z.; Safdar, M.; He, J., Component-Controllable WS_{2(1-x)}Se_{2x} Nanotubes for Efficient Hydrogen Evolution Reaction. *ACS Nano* **2014**, *8* (8), 8468-8476.
- Wang, H.; Kong, D.; Johannes, P.; Cha, J. J.; Zheng, G.; Yan, K.; Liu, N.; Cui, Y., MoSe₂ and WSe₂ Nanofilms with Vertically Aligned Molecular Layers on Curved and Rough Surfaces. *Nano Lett.* **2013**, *13* (7), 3426-3433.
- Eng, A. Y. S.; Ambrosi, A.; Sofer, Z.; Šimek, P.; Pumera, M., Electrochemistry of Transition Metal Dichalcogenides: Strong Dependence on the Metal-to-Chalcogen Composition and Exfoliation Method. *ACS Nano* **2014**, *8* (12), 12185-12198.
- Deng, J.; Li, H.; Xiao, J.; Tu, Y.; Deng, D.; Yang, H.; Tian, H.; Li, J.; Ren, P.; Bao, X., Triggering the Electrocatalytic Hydrogen Evolution Activity of the Inert Two-Dimensional MoS₂ Surface via Single-Atom Metal Doping. *Energy Environ. Sci.* **2015**, *8* (5), 1594-1601.
- Liu, Z.; Zhao, H.; Li, N.; Zhang, Y.; Zhang, X.; Du, Y., Assembled 3D electrocatalysts for efficient hydrogen evolution: WSe₂ layers anchored on graphene sheets. *Inorg. Chem. Front.* **2016**, *3* (2), 313-319.